Original Article
LncRNA H19 activates cell pyroptosis via the miR-22-3p/NLRP3 axis in pneumonia

Jiyang Sun[1], Shun Mao[2], Wei Ji[1]

[1]Department of Pediatric Pulmonology, Children's Hospital of Soochow University, Suzhou 215003, Jiangsu Province, China; [2]Department of Pneumology, The Fifth People's Hospital of Changshu, Changshu 215500, Jiangsu Province, China

Abstract: Objective: Pneumonia is an infectious pulmonary disease with a high morbidity and mortality. It has been reported that multiple long noncoding RNAs (LncRNAs) are involved in the progression of pneumonia, such as LncRNA SNHG16. However, the role and underlying mechanism of LncRNA H19 in the pyroptosis of pneumonia has not been elucidated. The purpose of this research was to explore the mechanism by which LncRNA H19 regulates LPS-induced pneumonia in WI-38 cells. Methods: An LPS induced pneumonia model in WI-38 cells was established. Total RNA extracted from WI-38 cells was analyzed using RT-qPCR, and the total proteins isolated from the WI-38 cells were analyzed using Western blotting. MTT assays, TUNEL staining, bioinformatics, and luciferase reporter assays were subsequently conducted. Results: In the LPS induced pneumonia model, LncRNA H19 silences inhibited LPS-induced WL-38 cell pyroptosis, and LncRNA H19 overexpression promotes LPS-induced WL-38 cell pyroptosis. Also, LncRNA H19 acts as a sponge of miR-22-3p, which targets NLRP3, and NLRP3 attenuates the effect of LncRNA H19 silencing on LPS-induced WL-38 cell pyroptosis. Conclusion: Our data demonstrated the roles and potential mechanisms of LncRNA H19 in the regulation of pneumonia cell pyroptosis, indicating that LncRNA H19 is an efficient predictive and curative target for pneumonia.

Keywords: Pneumonia, long noncoding RNA H19, MiR-22-3p, NLRP3, pyroptosis

Introduction

Pneumonia is an inflammatory infection of the lungs caused by multiple pathogenic infections, with a high mortality rate in children and elderly patients [1]. Its main symptoms are cough, fever, chest pain, and even respiratory failure [2]. At present, drug therapy is the main strategy for pneumonia treatment. Although with the emergence of new drugs and improvements in medical technology, some progress has been achieved. However, no effective drug has been found for pneumonia treatment due to the presence of various side effects, such as acute lung injury, bronchitis, etc. [1, 3, 4]. Therefore, determining the pathogenesis of pneumonia is beneficial in the search for effective therapeutic drugs and strategies. Also, an effective endotoxin, lipopolysaccharide (LPS), is essential for the inflammatory response associated with pneumonia [5]. Therefore, it is essential to explore the underlying mechanism of the LPS-induced inflammatory response and seek an effective treatment for pneumonia.

Pyroptosis is a new type of inflammatory programmed cell death, which depends on caspase-1 and gasdermin D (GSDMD) [6]. For the pyroptosis process, originally, the pro-pyroclastic prototype is triggered by the activation of the pro-inflammatory caspases, mainly caspase-1. Subsequently, GSDMD is cleaved by caspase-1 to mediate end-cell lysis, in which an active form of GSDMD consisting of an N-terminal domain is assembled to form pores in the cell membrane. Furthermore, these pores cause the rupture of the membrane, thus resulting in cell death. Concurrently, it causes excessive secretions of the IL-1β and IL-18 inflammatory cytokines, resulting in an inflammatory response [7-9]. Collectively, the GSDMD-N and casapse-1 protein levels indicate the degree of pyroptosis, and the IL-1β and IL-18 levels may indicate the inflammatory response severity. Also, it has been reported that NLRP3 inflammasome activation is an essential factor for promoting pyroptosis [10]. NLRP3 (NLR family pyrin domain containing 3), apoptosis-related speckle-like protein 1 (ASC-1), and caspase-1

form the NLRP3 inflammasome which has a positive effect on pneumonia progression [11]. Therefore, further investigation of the NLRP3 inflammasome provides novel insights into the development and progression of pneumonia.

Long non-coding RNAs (LncRNAs) are vital intracellular regulatory molecules, which have functional activity in various physiological processes [12]. LncRNA H19 belongs to the highly conserved imprinted gene cluster, and its regulatory function in cell biological activity has been reported, including proliferation, apoptosis and pyroptosis etc. It is worth noting that LncRNA acts as a competitive endogenous RNA (ceRNA), which regulates other RNA transcripts by contending against shared miRNA. For example, LncRNA H19 regulates the proliferation of ectopic endometrial cells by regulating miR-124-3p to target ITGB3 [13]. LncRNA H19 inhibits the apoptosis of hepatocellular carcinoma cells by activating the miR-193b/MAPK1 axis [14]. Also, LncRNA H19 promotes Hep3B cell pyroptosis by targeting miR-15b by activating the CDC42/PAK1 pathway [15]. On the other hand, multiple LncRNAs are involved in the progression of pneumonia, such as LncRNA SNHG16 and LncRNA HAGLROS [1, 16]. However, the roles of LncRNA H19 in the pyroptosis of pneumonia remain unclear.

The aim of this paper was to investigate the effect of LncRNA H19 on the pyroptosis of LPS-induced WI-38 cells and its related mechanisms. Our findings may provide new therapeutic biomarkers for predicting the progression and prognosis of pneumonia.

Materials and methods

Cell lines and culture

WI-38 cells were provided by Yunnan University (Yunnan, China). Dulbecco's modified Eagle's medium (DMEM, Roche, Basel, Switzerland) supplemented with 1% penicillin-streptomycin solution and 10% fetal bovine serum (FBS) (Solarbio, Beijing, China) was used to culture the cells in a humid incubator containing 5% CO_2 at 37°C.

Cell transfection

Sangon Biotech (Shanghai, China) synthesized the random sequences of si-LncRNA H19, and the miR-22-3p mimics/inhibitor and the si-

NLRP3, si-NC, NC-mimics, and NC-inhibitor served as negative controls. The plasmids Lv-LncRNA H19 were synthesized by Sangon Biotech (Shanghai, China). Lipofectamine™ 3,000 Transfection Reagent (Takara, Liaonin, China) was used to transfect the plasmids. Following 72 h of transfection, WI-38 cells were used in the subsequent experiments.

Drugs and antibodies

Phalloidin, ethanol, proteinase K, 4', 6-dimid-2-phenylindoles, and lipopolysaccharide (LPS) were purchased from Soleil (Beijing, China, purity ≥98%). Antibodies against the GSDMD, NLRP3, ASC-1 and cleaved Caspase-1 were obtained from Roche (Basel, Switzerland).

Pneumonia cell model

For the LPS-induced pneumonia model in vitro, 0 μg/mL, 5 μg/mL, 10 μg/mL, and 20 μg/mL LPS was used to treat the WI-38 cells for 24 h, respectively. MTT was performed to determine the cell proliferation. TUNEL staining was carried out to assess the pyroptosis. RT-qPCR and Western blot analyses were conducted to measure the pyroptosis-related gene expressions, including GSDMD-N, IL-1β, and IL-18. The GSDMD-N levels indicate the pyroptosis degree, and the IL-1β and IL-18 levels indicate the severity of the inflammatory response.

RT-qPCR

TRIzol reagent (Takara, Liaonin, China) was used to extract the total RNA from the WI-38 cells which were treated with a corresponding dose of LPS and transfected with corresponding plasmids. An M-MLV Reverse Transcriptase (RNase H) kits (Takara, Liaoning, China) were used to synthesize the cDNA. RT-qPCR was performed as previously described [17]. The primers used in this research are shown in **Table 1**.

Western blot

Total proteins were isolated from the WI-38 cells which were treated with a corresponding dose of LPS and transfected with the corresponding plasmids using a cell lysis buffer (Beyotime, Nanjing, China). Western blots were performed as previously described [18]. All the antibodies used in this research were obtained from Abcam (Cambridge, England, 1:1,000), GSDMD-N (ab215203), GSDMD (ab219800),

Table 1. Primer sequences

Primer name	(5'-3') Primer sequences
F-GSDMD	5'-GTGCCTCCACAACTTCCTGA-3'
R-GSDMD	5'-GTCTCCACCTCTGCCCGTAG-3'
F-IL-1β	5'-CTCGTGCTGTCGGACCCAT-3'
R-IL-1β	5'-CAGGCTTGTGCTCTGCTGTG-3'
F-IL-18	5'-ATCGGCCTCTATTTGAAGATATG-3'
R-IL-18	5'-TCACAGAGATAGTTACAGCCATACC-3'
F- LncRNA H19	5'-GCGGGTCTGTTTCTTTACTTCC-3'
R- LncRNA H19	5'-CTTTGATGTTGGGCTGATGAGG-3'
F-NLRP3	5'-CCACAAGATCGTGAGAAAACCC-3'
R-NLRP3	5'-CGGTCCT ATGTGCTCGTCA-3'
F-ASC-1	5'-TGGATGCTCTGTACG GGAAG-3'
R-ASC-1	5'-CCAGGCTGGTGTGAAACTGAA-3'
F-Caspase-1	5'-CAGACAAGGGTGCTGAACAA-3'
R-Caspase-1	5'-CGGAATAACGGAGTCAATCA-3'
F-miR-22-3p	5'-GTTCTTCAGTGGCAAGC-3'
R-miR-22-3p	5'-GAACATGTCTGCGTATCTC-3'
F-GAPDH	5'-GAGTCAACGGATTTGGTCGT-3'
R-GAPDH	5'-TTGATTTTGGAGGGATCTCG-3'
F-U6	5'-CTCGCTTCGGCAGCACA-3'
R-U6	5'-AACGCTTCACGAATTTGCGT-3'

NLRP3 (ab263899), ASC-1 (ab70627), Caspase-1 (ab179515), cleaved Caspase-1 (ab-32042) and β-actin (ab8226). The optical densities of the protein bands were quantified using ImageJ software (ImageJ Software, Inc.).

MTT assay

The 3-(4,5-dimethylthiazol-2-yl)-2,5-diphenyltetrazolium bromide (MTT, Roche, Basel, Switzerland) assays were performed to assess the cell viability. In detail, $1×10^4$ WI-38 cells which were treated with corresponding doses of LPS and transfected with the corresponding plasmids were seeded in 96-well plates and incubated with 20 µL of MTT reagent (5 mg/mL) for 6 h at 37°C. After removing the medium, 150 µL of dimethyl sulfoxide (DMSO, Roche, Basel, Switzerland) was added. A Microplate Reader (Olympus, Tokyo, Japan) was used to evaluate the cell viability at 570 nm absorbance.

TUNEL staining

The TUNEL assays were conducted according to the instructions provided by Vanzyme (Nanjing, China), with minor modifications [16].

Immunofluorescence

The immunofluorescence assays were done as described with minor modifications [19]. In detail, $1×10^5$ WI-38 cells which were treated with corresponding doses of LPS and transfected with corresponding plasmids and then seeded in 12-well plates, washed with 1×PBS and fixed for 15 min in 3.7% formaldehyde. The GSDMD-N protein expression was determined using GSDMD-N antibodies (Roche, Basel, Switzerland, 1:1,000) and Alexa Fluor®568 Goat Anti-Mouse (IgG) (Roche, Basel, Switzerland, 1:2,000). Subsequently, the labeled cells were incubated with the phalloidin (Soleil, China, Beijing, 1:40) in 1×PBS for 1 h at 37°C. Further, the cells were washed with 1×PBS and incubated with 4', 6-dimid-2-phenylindoles (DAPI) (Soleil, Beijing, China, 1:1,000) for 5 min. Finally, the cells were imaged using an Olympus 71 inverted fluorescence microscope (IX61, Olympus, Tokyo, Japan).

Subcellular fractionation analysis

PARIS™ kits (Invitrogen, Waltham, USA) were used for the subcellular fractionation analyses, according to the instructions. Nuclear and cytoplasmic extraction reagents (Beyotime, Nanjing, China) were used to separate the cytoplasms and nuclear grades from the WI-38 cells. RT-qPCR was conducted to analyze the cytoplasmic and nuclear RNA extracts, GAPDH and U6 served as normalizing controls, respectively.

ELISA

Following the treatment with the corresponding doses of LPS and the transfection with the corresponding plasmids, 1 mL of protein extraction reagent (Beyotime, Nanjing, China) was used to lyse the WI-38 cells. Subsequently, the inflammatory factor IL-1β and IL-18 levels in the WI-38 cell supernatant were determined according to the instructions using an ELISA kit (Roche, Basel, Switzerland).

Bioinformatics and luciferase reporter assays

TargetScan was used to predict the underlying target genes. Dual luciferase reporter assays were carried out to confirm the target genes of miR-22-3p and NLRP3. Briefly, the NLRP3 or its mutant (Mut) fragment and 3'UTR-WT or 3'UTR-

MUT of NLRP3 were amplified and sub-cloned into a pGL4.10 luciferase reporter vector. The wild-type or mutant NLRP3 plasmids (500 ng) were transfected into the cells in each well of 6-well plates. MiR-22-3p mimics (100 nM) and NC mimics (100 nM) were co-transfected into the WI-38 cells using the Lipofectamine™ 3000 (Roche, Basel, Switzerland) according to the manufacturer's instructions. The luciferase activity was assessed using the Dual-Light Chemiluminescent Reporter Gene Assay System (Applied Biosystems, Foster City, USA) and normalized using Renilla luciferase activity. The dual-luciferase reporter assays were carried as previously described [20].

Statistical analysis

All the data, which were presented as the means ± standard deviations ($\bar{x}$ ± sd) of three independent experiments, were statistically analyzed using GraphPad Prism version 5.0 software (GraphPad Software, Inc.). Student's t tests or one-way ANOVA followed by Tukey post-hoc tests were used for the comparisons between two groups or among multiple groups. When the *P* value was <0.05, the difference was considered statistically significant.
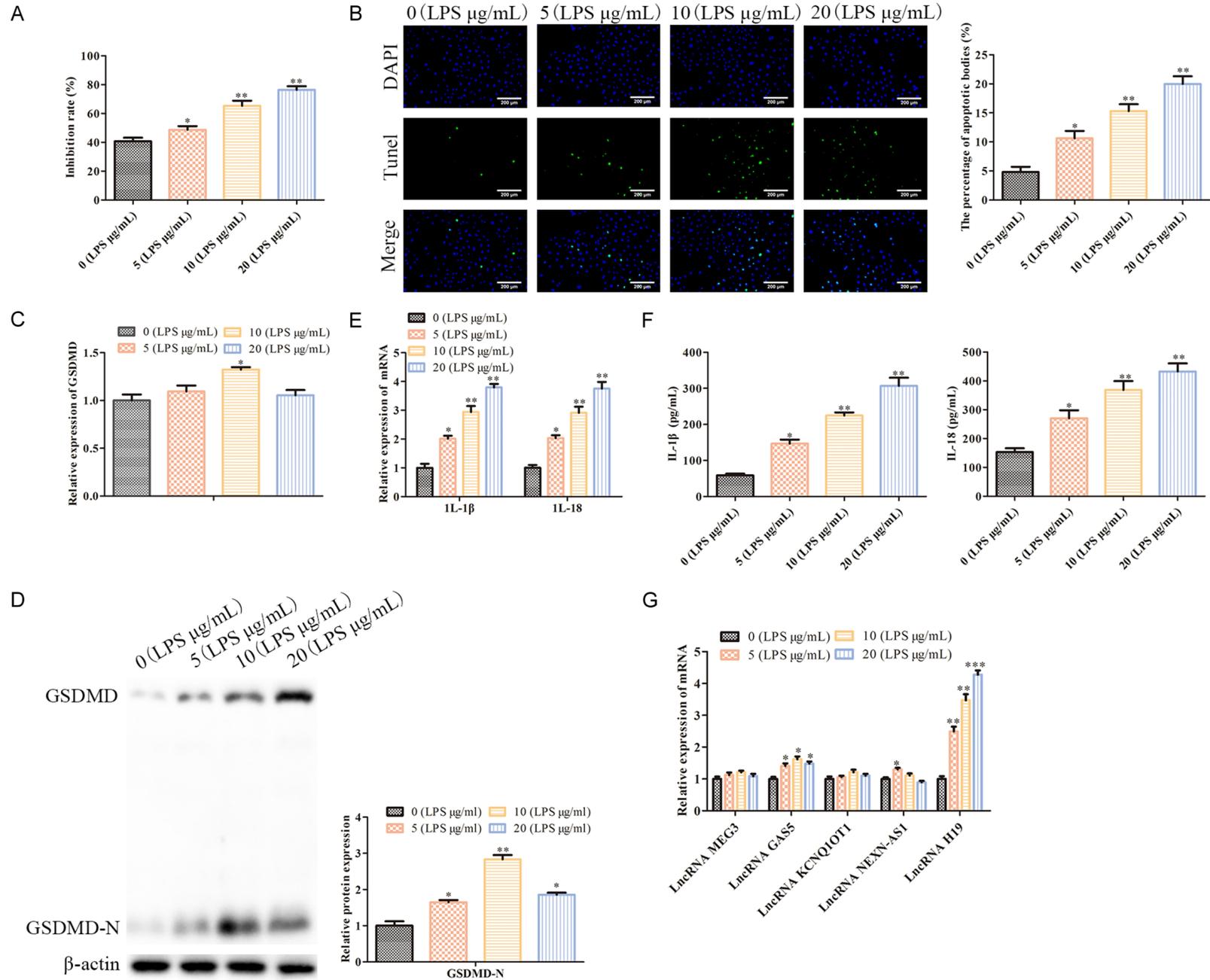
Results

LPS induced a pneumonia model in vitro

To verify whether LPS successfully induced a pneumonia model *in vitro*, our MTT assay analysis showed that LPS dose-dependently inhibited WI-38 cell proliferation (P<0.05; **Figure 1A**). The TUNEL staining indicated that LPS dose-dependently promoted WI-38 cell pyroptosis (P<0.05; **Figure 1B**). As shown in **Figure 1C** and **1D**, LPS had no effect on the mRNA level of GSDMD, but it dose-dependently promoted GSDMD-N protein expression (P<0.05). Additionally, GSDMD served as a pyroptosis-related protein, and its N-terminal cleavage indicated the occurrence of pyroptosis. Further, our RT-qPCR and ELISA analyses showed that LPS dose-dependently up-regulated the IL-1β and IL-18 levels in the supernatant of the WI-38 cells (P<0.05; **Figure 1E** and **1F**). Moreover, the prominent feature of pyroptosis is that activated Caspase-1 mediates the pro-inflammatory signals, including the IL-1β and IL-18 inflammatory factors, thereby initiating body immunity. Therefore, the IL-1β and IL-18 levels indicate

the degree of pyroptosis [21]. Based on the above data, we believe that LPS successfully induced a pneumonia model *in vitro*. Also, our RT-qPCR analysis showed that LPS dose-dependently promotes the LncRNA H19 levels, which have been reported to be associated with pyroptosis [22] (P<0.05; **Figure 1G**). These data indicate that LncRNA H19 may participate in the regulation of WI-38 cell pyroptosis.

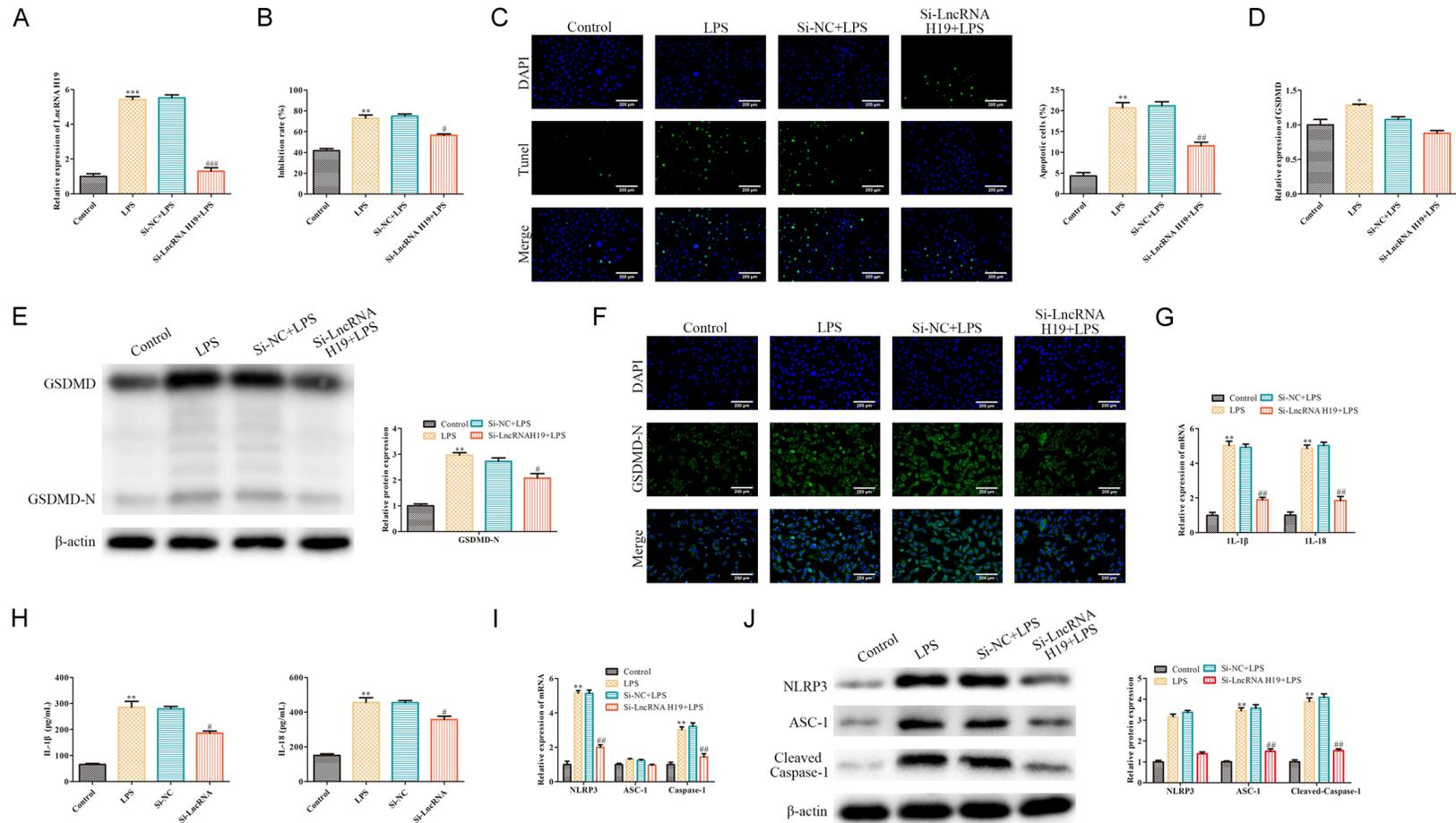*LncRNA H19 silencing inhibited LPS-induced WL-38 cell pyroptosis*

To investigate whether LncRNA H19 had any effect on the cell pyroptosis, LPS-induced WL-38 cells were transfected with si-LncRNA H19 to knockdown LncRNA H19. The RT-qPCR analysis indicated that LPS promotes LncRNA H19 expression in WI-38 cells, which was antagonized by the LncRNA H19 silencing (P<0.05; **Figure 2A**). The MTT assays indicated that LPS inhibited the WI-38 cell proliferation, which was alleviated by the LncRNA H19 silencing (P<0.05; **Figure 2B**). The TUNEL staining showed that the WI-38 cell pyroptosis induced by LPS was inhibited by the LncRNA H19 silencing (P<0.05; **Figure 2C**). Furthermore, as shown in **Figure 2D** and **2E**, the GSDMD-N expression induced by LPS was inhibited by the LncRNA H19 silencing (P<0.05). Immunofluorescence further confirmed this phenomenon (P<0.05; **Figure 2F**). Furthermore, our RT-qPCR and ELISA analyses showed that the IL-1β and IL-18 levels induced by LPS were inhibited by the LncRNA H19 silencing in the WI-38 cells (P<0.05; **Figure 2G** and **2H**). NLRP3 regulates the activation of Caspase-1, thereby promoting the maturation and secretion of the cytokine precursors pro-IL-1β and pro-IL-18, which in turn regulate the caspase-1 dependent pyroptosis [23]. In addition, ASC-1, which serves as a Caspase-1-associated speck-like protein in inflammasomes, plays a vital role in pyroptosis. To explore the effect of the LncRNA H19 silencing on the NLRP3/ASC-1/Caspase-1 axis in LPS-induced WI-38 cells, our RT-qPCR and Western blot analyses indicated that the NLRP3, ASC-1 and Caspase-1 levels induced by LPS were inhibited by the LncRNA H19 knockdown in the WI-38 cells (P<0.05; **Figure 2I** and **2J**), indicated that LncRNA H19 is an essential factor involved in WI-38 cell pyroptosis. Taken together, LncRNA H19 silencing inhibits LPS-induced WL-38 cell pyroptosis.

LncRNA H19 and the progression of pneumonia

Figure 1. LPS induces a pneumonia model in vitro. A: MTT assays were conducted to evaluate the cell proliferation; *P<0.05, **P<0.01, vs. 0 (LPS µg/mL). B: TUNEL staining (100×) was performed to assess the cell pyroptosis; *P<0.05, **P<0.01, vs. 0 (LPS µg/mL). C: RT-PCR was carried out to determine the GSDMD mRNA levels in the WI-38 cells; *P<0.05, vs. 0 (LPS µg/mL). D: Western blot analysis was conducted to measure the GSDMD-N protein expressions in the WI-38 cells. *P<0.05, **P<0.01, vs. 0 (LPS µg/mL). E: RT-A PCR analysis was performed to measure the mRNA levels of the IL-1β and IL-18 genes in the WI-38 cells. *P<0.05, **P<0.01, vs. 0 (LPS µg/mL). F: ELISA assays were carried to assess the IL-1β and IL-18 levels in the WI-38 cell supernatant. *P<0.05, **P<0.01, vs. 0 (LPS µg/mL). G: An RT-qPCR analysis was performed to measure the mRNA levels of the LncRNAs which are related to the pyroptosis, including LncRNA MEG3, LncRNA GAS5, LncRNA kcnq1ot1, LncRNA NEXN-AS1 and LncRNA H19. *P<0.05, **P<0.01, ***P<0.001, vs. 0 (LPS µg/mL).

Figure 2. LncRNA H19 silencing inhibited the LPS-induced WL-38 cell pyroptosis. A: RT-qPCR was conducted to assess the transfection efficiency; ***P<0.001, LPS vs. the control; ###P<0.001, Si-LncRNA H19+LPS vs. Si-NC+LPS. B: MTT assays were performed to evaluate the WI-38 cell proliferation; **P<0.01, LPS vs. control; #P<0.05, Si-LncRNA H19+LPS vs. Si-NC+LPS. C: TUNEL staining was carried out to assess the WI-38 cell pyroptosis (100×); **P<0.01, LPS vs. control; ##P<0.01, Si-LncRNA H19+LPS vs. Si-NC+LPS. D, E: RT-qPCR and Western blot were conducted to determine the GSDMD and GSDMD-N levels in the WI-38 cells, respectively; *P<0.05, **P<0.01, LPS vs. the control; #P<0.05, Si-LncRNA H19+LPS vs. Si-NC+LPS. F: Immunofluorescence was carried to evaluate the GSDMD-N protein fluorescence intensity in the WI-38 cells (100×). G, H: The IL-1β and IL-18 levels in the WI-38 cells; **P<0.01, LPS vs. the control; #P<0.05, ##P<0.01, Si-LncRNA H19+LPS vs. Si-NC+LPS. I, J: The NLRP3, ASC-1, Caspase-1 levels in the WI-38 cells. **P<0.01, LPS vs. the control; ##P<0.01, Si-LncRNA H19+LPS vs. Si-NC+LPS.

LncRNA H19 overexpression promoted LPS-induced WL-38 cell pyroptosis

To further verify the above conclusions, LPS-induced WL-38 cells were transfected with Lv-LncRNA H19 for LncRNA H19 overexpression. An RT-qPCR analysis indicated that LncRNA H19 was overexpressed in the LPS-induced WI-38 cells (P<0.05; **Figure 3A**). An MTT assay analysis indicated that LncRNA H19 overexpression aggravated the LPS induced WI-38 cell proliferation inhibition (P<0.05; **Figure 3B**). The TUNEL staining indicated that LncRNA H19 overexpression promotes the WI-38 cell pyroptosis induced by LPS (P<0.05; **Figure 3C**). As shown in **Figure 3E**, LncRNA H19 overexpression promoted GSDMD-N protein expression in the LPS-treated WI-38 cells (P<0.05). This phenomenon was further confirmed using an immunofluorescence analysis (P<0.05; **Figure 3F**). Furthermore, the RT-qPCR and ELISA analyses indicated that the LncRNA H19 overexpression up-regulated the IL-1β and IL-18 levels secreted by the LPS-treated WI-38 cells (P<0.05; **Figure 3G** and **3H**). In addition, the LncRNA H19 overexpression up-regulated the NLRP3, ASC-1, and Caspase-1 levels induced by LPS in the WI-38 cells (P<0.05; **Figure 3I** and **3J**). Collectively, the LncRNA H19 overexpression promoted the LPS-induced WL-38 cell pyroptosis.

LncRNA H19 served as a sponge of miR-22-3p which targets NLRP3

As is known, LncRNA H19 is extensively involved in the regulation of disease progression [24]. To confirm the downstream effects of LncRNA H19 in LPS-treated WI-38 cells, a subcellular fractionation analysis showed that LncRNA H19 was localized in the cytoplasms and nuclei of the WI-38 cells (**Figure 4A**), indicating that LncRNA H19 may play a role in pneumonia via the ceRNA regulatory network. Our bioinformatics analysis indicated that miR-22-3p is the tar-

get of both LncRNA H19 and NLRP3 (P<0.05; **Figure 4B**), indicating that the LncRNA H19/miR-22-3p/NLRP3 axis may participate in the regulation of the pneumonia progression. Subsequently, the RT-qPCR analysis revealed that LPS dose-dependently inhibited the miR-22-3p expression in the WI-38 cells (P<0.05; **Figure 4C**). The bioinformatics analysis indicated that a putative interaction occurred between LncRNA H19 and miR-22-3p (**Figure 4D**). As shown in **Figure 4E**, miR-22-3p was overexpressed in the LPS-induced WI-38 cells (P<0.05). The luciferase reporter assay confirmed that the miR-22-3p mimics decreased the luciferase activity of WT LncRNA H19 in the LPS-treated WI-38 cells, but this inhibition was blocked when the putative binding sites were mutated (P<0.05; **Figure 4F**). Also, our RT-qPCR analysis showed that the miR-22-3p levels inhibited by LPS were rescued by the LncRNA H19 silencing (P<0.05; **Figure 4G**). The above findings show that LncRNA H19 may affect the deregulation of miR-122-3p through the sponging action. Furthermore, analogously, the bioinformatics analysis, the luciferase reporter assay, and the RT-qPCR and Western blot analyses showed that miR-22-3p targeted and negatively regulated NLRP3 (P<0.05; **Figure 4H-K**). Functionally, the RT-qPCR and Western blot analysis indicated that the pyroptosis related proteins levels, including GSDMD-N, NLRP3, ASC-1, Caspase-1 and cleaved Caspase-1 inhibited by the LncRNA H19 silencing were rescued by the miR-22-3p inhibition (**Figure 4L**, **4M**). These data indicate that LncRNA H19 may regulate LPS-induced WI-38 cell pyroptosis via the miR-22-3p/NLRP3 axis.

MiR-22-3p/NLRP3 axis attenuated the effect of LncRNA H19 silencing on the LPS-induced WL-38 cell pyroptosis

To further explore NLRP3's roles in WI-38 cell pyroptosis, LPS-treated WL-38 cells, in which LncRNA H19 was inhibited, were transfected
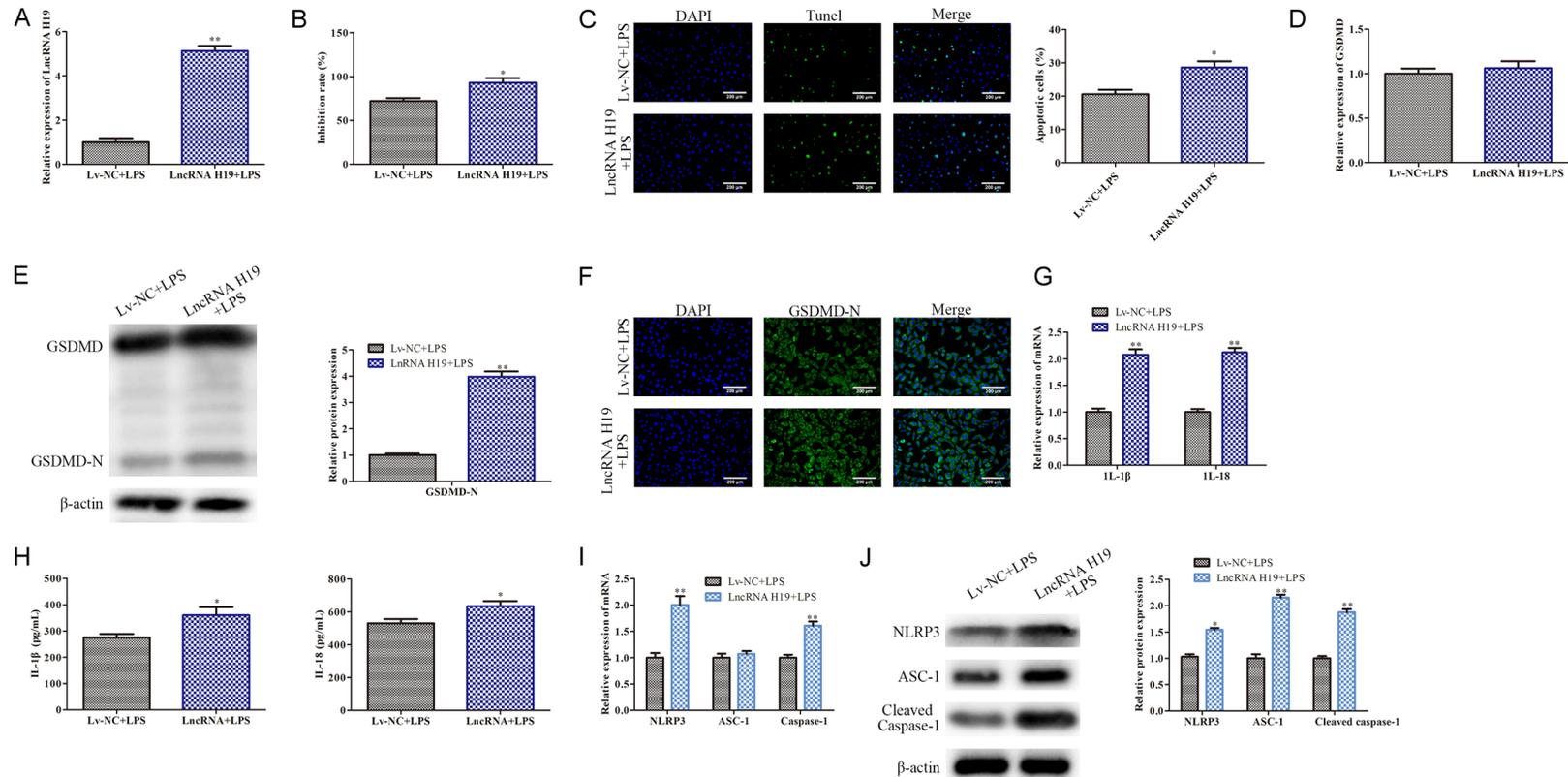
Figure 3. LncRNA H19 overexpression promotes LPS-induced WL-38 cell pyroptosis. A: An RT-qPCR analysis was carried out to determine the LncRNA H19 expression in the WI-38 cells; **P<0.01, LncRNA H19+LPS vs. Lv-NC+LPS. B: MTT assays were conducted to evaluate the WI-38 cell proliferation; *P<0.05, LncRNA H19+LPS vs. Lv-NC+LPS. C: TUNEL staining was carried our to assess the WI-38 cell pyroptosis (100×); *P<0.05, LncRNA H19+LPS vs. Lv-NC+LPS. D, E: The GS-DMD and GSDMD-N levels in the WI-38 cells; **P<0.01, LncRNA H19+LPS vs. Lv-NC+LPS. F: Immunofluorescence was performed to assess the GSDMD-N protein fluorescence intensity in the WI-38 cells (100×); G, H: The IL-1β and IL-18 levels in the WI-38 cells; *P<0.05, **P<0.01, LncRNA H19+LPS vs. Lv-NC+LPS. I, J: The NLRP3, ASC-1, and Caspase-1 levels. *P<0.05, **P<0.01, LncRNA H19+LPS vs. Lv-NC+LPS.
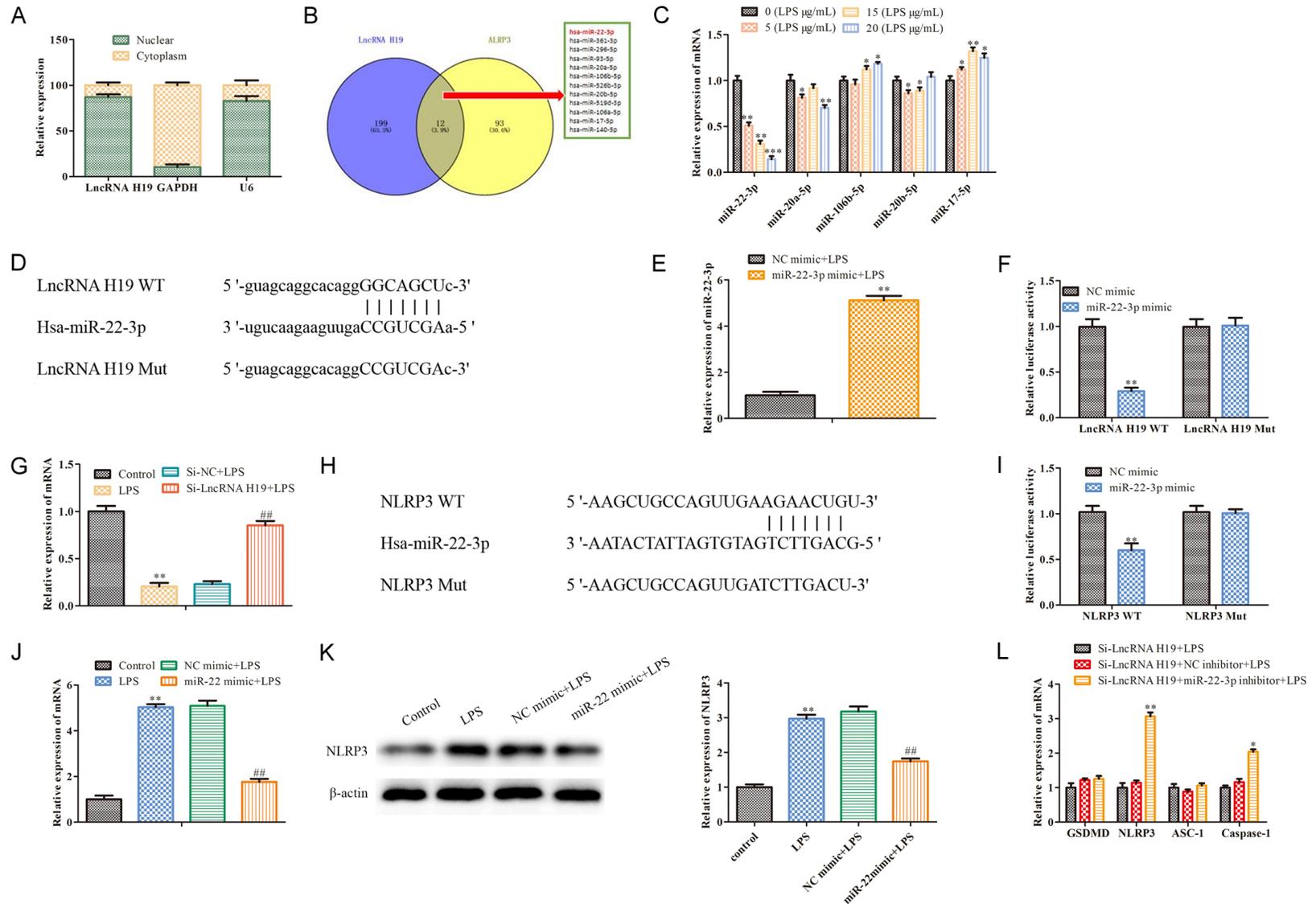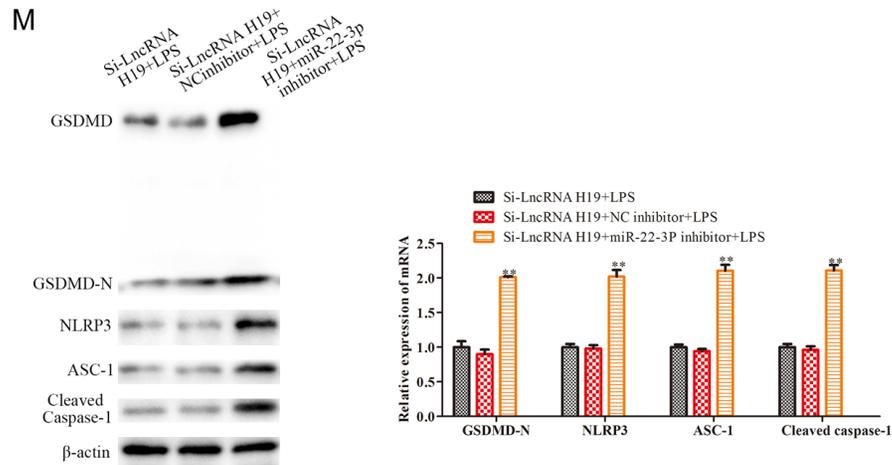
Figure 4. MiR-22-3p which is the target of LncRNA H19, targets NLRP3. A: A subcellular fractionation analysis was performed to determine the localization of LncRNA H19 in the WI-38 cells; B: Bioinformatics analysis indicated miR-22-3p is the target of LncRNA H19 and NLRP3; C: RT-qPCR was carried our to assess the levels of the miRNAs in the LPS induced WI-38 cells, including miR-22-3p, miR-20a-5p, miR-106b-5p, miR-20b-5p, and miR-17-5p; $^{*}P<0.05$, $^{**}P<0.01$, vs. 0 (LPS μg/mL). D: TargetScan software was used to predict the potential binding site between LncRNA H19 and miR-22-3p. E: RT-qPCR was conducted to assess the miR-22-3p expression; $^{**}P<0.01$, vs. NC mimic+LPS. F: A dual luciferase reporter gene assay was performed to confirm the direct binding relationship between LncRNA H19 and miR-22-3p. $^{**}P<0.01$, vs. NC mimic. G: RT-qPCR was performed to assess the miR-22-3p expression; $^{**}P<0.01$, LPS vs. the control; $^{##}P<0.01$, Si-LncRNA H19+LPS vs. Si-NC+LPS. H: TargetScan software was used to predict the potential binding site between miR-22-3p and NLRP3. I: A dual luciferase reporter gene assay was conducted to confirm the direct binding relationship between miR-22-3p and NLRP3. $^{**}P<0.01$, vs. the NC mimic. J: RT-qPCR was carried out to assess the NLRP3 mRNA levels. $^{**}P<0.01$, LPS vs. the control; $^{##}P<0.01$, miR-22 mimic+LPS vs. the NC mimic+LPS. K: Western blot was performed to measure the NLRP3 protein expression. $^{**}P<0.01$, LPS vs. the control; $^{##}P<0.01$, miR-22 mimic+LPS vs. NC mimic+LPS. L, M: The pyroptosis-related gene levels were measured using RT-qPCR and Western blot, including GSDMD, GSDMD-N, NLRP3, ASC-1 and Caspase-1. $^{*}P<0.05$, $^{**}P<0.01$, Si-LncRNA H19+miR-22-3p inhibitor+LPS vs. Si-LncRNA H19+NC inhibitor+LPS.

with si-NLRP3 for NLRP3 silencing, with si-NC serving as a negative control. Our RT-qPCR and Western blot analyses showed that the NLRP3 levels were effectively silenced in the LPS-induced WI-38 cells, in which LncRNA H19 was inhibited, following the transfection with si-NLRP3, compared with the control (P<0.05; **Figure 5A**). An MTT assay analysis showed that the miR-22-3p inhibitor inhibited the LPS-treated WI-38 cell proliferation which was transfected with si-LncRNA H19, but the NLRP3 silencing attenuated this inhibitory effect (P<0.05; **Figure 5B**). As shown in **Figure 5C**, miR-22-3p inhibitor promoted the pyroptosis of the LPS-treated WI-38 cells with LncRNA H19 knockdown (P<0.05). Furthermore, the RT-qPCR and Western blot analyses indicated that the GSDMD-N, NLRP3, ASC-1, Caspase-1 and Cleaved Caspase-1 levels in the LPS-treated WI-38 cells in which LncRNA H19 was inhibited, were up-regulated by the miR-22-3p inhibitor, but this upward trend was inhibited by the NLRP3 silencing (P <0.05; **Figure 5D** and **5E**). Additionally, the RT-qPCR and ELISA analyses indicated that the miR-22-3p inhibitor promoted the IL-1β and IL-18 levels in the LPS-treated WI-38 cells which inhibited LncRNA H19, but this facilitating effect was antagonized by the NLRP3 silencing (P<0.05; **Figure 5F** and **5G**). Combining these results, the miR-22-3p/NLRP3 axis attenuated the LncRNA H19 silencing effect on the LPS-induced WL-38 cell pyroptosis, indicating that LncRNA H19 may regulate LPS-induced WI-38 cell pyroptosis via the miR-22-3p/NLRP3 axis.
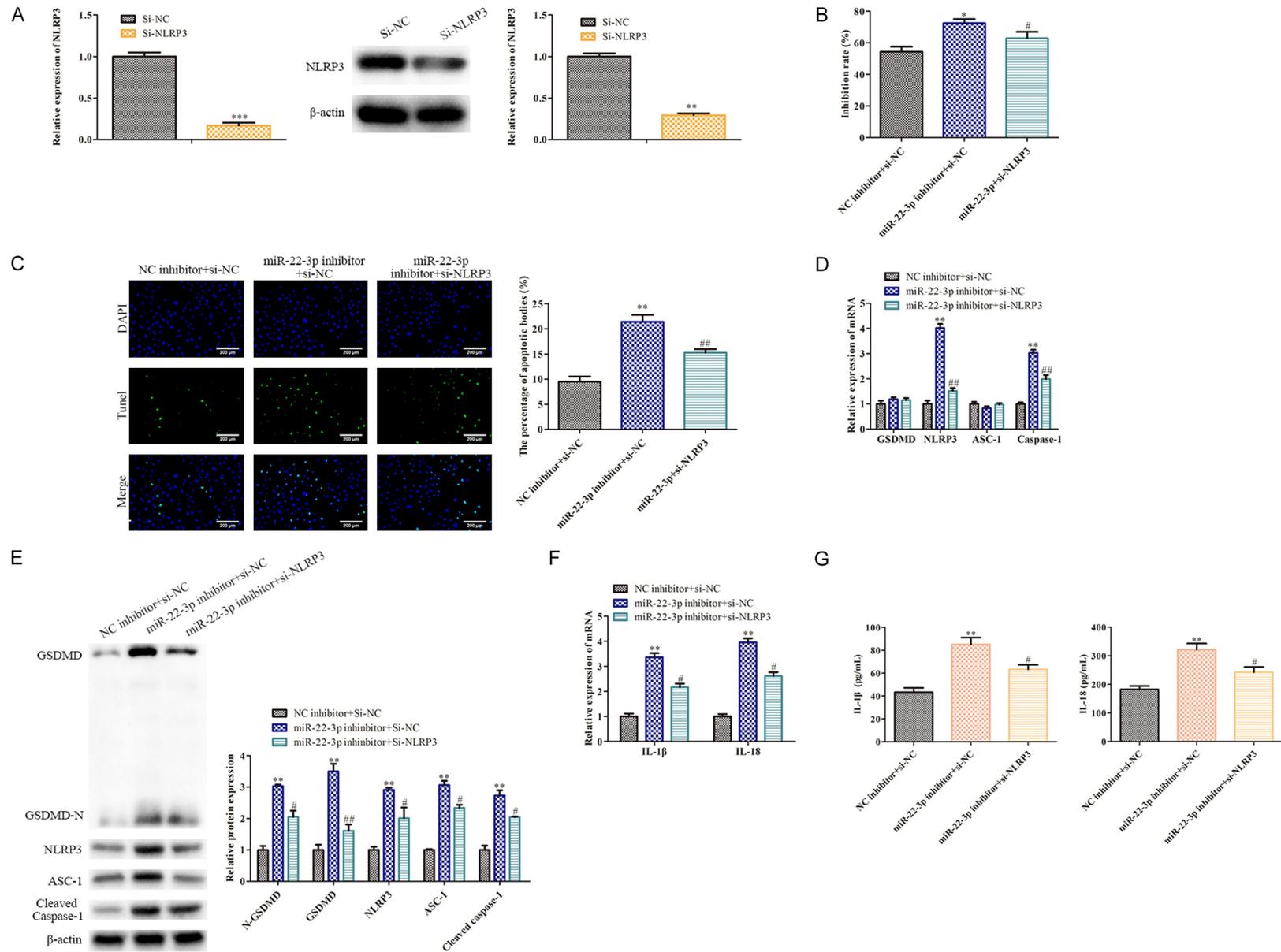
Discussion

Pneumonia is one of the deadliest respiratory infections, with a high morbidity and mortality, especially in children and the elderly [25]. Increasing evidence indicates that LncRNAs are involved in the regulation of pneumonia progression [26]. Therefore, the identification of the key LncRNAs may contribute to developing effective targets for pneumonia treatment. In the present study, our findings indicate that pyroptosis participates in an LPS induced pneumonia model of WI-38 cells. To take a deep look at the regulatory mechanisms, five LncRNAs that are reported to promote pyroptosis were selected to examine their relative expression levels. Among them, the expressions of MEG3, GAS5, KCNQ1OT1 and NEXN-AS1 exhib-

ited little variation [27-30]. On the other hand, H19 was increased significantly after LPS induction [22]. Furthermore, LncRNA H19 silencing inhibited the LPS-induced WL-38 cell pyroptosis, and LncRNA H19 overexpression promoted LPS-induced WL-38 cell pyroptosis. Also, LncRNA H19 serves as a sponge of miR-22-3p which targets NLRP3, and NLRP3 attenuates the effect of LncRNA H19 silencing on LPS-induced WL-38 cell pyroptosis. Collectively, LncRNA H19 regulates the LPS-induced WI-38 cell pyroptosis via the miR-22-3p/NLRP3 axis. Our data demonstrated the roles and underlying mechanisms of LncRNA H19 in the regulation of pneumonia cell pyroptosis, indicating that LncRNA H19 may be a promising predictive and therapeutic target for pneumonia.

Studies show that LncRNAs are involved in the regulation of the progression of various diseases in multiple ways [24]. Also, LncRNAs, which act as ceRNAs regulate other RNA transcripts by competing for shared miRNA. For example, the LncRNA H19/microRNA-675/PPARα axis regulates hepatitis B virus protein-induced hepatocyte injury via the Akt/mTOR pathway [12]. LncRNA H19 prevents obesity-induced myocardial injury through the miR-29a/IGF-1 axis [31]. Also, LncRNA H19 up-regulates PTEN via miR-152-3p to promote wound healing in DFU [32]. Our findings show that LncRNA H19 is highly expressed in pneumonia and is associated with the LPS-induced pyroptosis of WI-38 cells. Notably, the LncRNA H19 silencing attenuates the inhibitory effect of LPS on the proliferation, and inhibits the LPS-induced WI-38 cell pyroptosis because the levels of the pyroptosis-related proteins were decreased, including GSDMD-N, IL-1β, IL-18, NLRP3, ASC-1, Caspase-1 and cleaved Caspase-1 and vice versa. These findings indicate that LncRNA H19 plays a positive role in LPS-induced WI-38 cell pyroptosis.

MicroRNAs (miRNAs) are defined as a group of non-coding RNA sequences of approximately 18-25 bp [33]. It has been well-documented that miRNAs play essential roles in gene expression via multiple mechanisms, such as transcription modulation; thus, miRNAs are crucial regulators for diverse molecular and cellular activities, impacting numerous physiological and pathological processes [6, 34]. For example, multiple miRNAs are involved in the regula-

Figure 5. NLRP3 attenuates the effect of LncRNA H19 on the LPS-induced WL-38 cell pyroptosis. A: RT-qPCR and Western blot were conducted to assess the NLRP3 levels; **P<0.01, ***P<0.001, vs. Si-NC. B: MTT assays were performed to evaluate the WI-38 cell proliferation; *P<0.05, miR-22-3p inhibitor+NC vs. NC inhibitor+si-NC; #P<0.05, miR-22-3p+si-NLPR3 vs. miR-22-3p inhibitor+si-NC. C: TUNEL staining was carried to measure the WI-38 cell pyroptosis (100×); **P<0.01, miR-22-3p inhibitor+NC vs. NC inhibitor+si-NC; ##P<0.01, miR-22-3p+si-NLPR3 vs. miR-22-3p inhibitor+si-NC. D, E: RT-qPCR and Western blot were conducted to measure the levels of the pyroptosis-related genes, including GSDMD, GSDMD-N, NLRP3, ASC-1 and Caspase-1; **P<0.01, miR-22-3p inhibitor+NC vs. NC inhibitor+si-NC; #P<0.05, ##P<0.01, miR-22-3p+si-NLPR3 vs. miR-22-3p inhibitor+si-NC. F, G: RT-qPCR and ELISA analyses were performed to assess the IL-1β and IL-18 levels. **P<0.01, miR-22-3p inhibitor+NC vs. NC inhibitor+si-NC; #P<0.05, miR-22-3p+si-NLPR3 vs. miR-22-3p inhibitor+si-NC.

tion of pneumonia progression, including miR-1247, miR-297 [5, 16, 35]. LncRNA H19 serves as a sponge of miR-22-3p which targets NLRP3, and NLRP3 attenuates the effect of LncRNA H19 silencing on LPS-induced WL-38 cell pyroptosis. LncRNA H19 regulates LPS-induced WI-38 cell pyroptosis via the miR-22-3p/NLRP3 axis. Our results indicate that miR-22-3p is highly expressed in lung tissues, and its expression is inhibited in LPS-induced WI-38 cells. Further, miR-22-3p functions as a sponge of LncRNA H19 and targets the 3'UTR of NLRP3. The LncRNA H19 silencing-induced inhibition of the expression levels of the pyroptosis related proteins, including GSDMD-N, NLRP3, ASC-1, Caspase-1 and cleaved Caspase-1 are rescued by the miR-22-3p knockdown. In addition, NLRP3 attenuates the effect of LncRNA H19 silencing on LPS-induced WL-38 cell pyroptosis. These findings indicate that LncRNA H19 may activate the LPS-induced WI-38 cell pyroptosis via the miR-22-3p/NLRP3 axis. More work should be carried out to explore the function of the miR-22-3p/NLRP3 axis.

There are some limitations to this work. The exact mechanism of the miR-22-3p/NLRP3 axis function is still unclear, so it should be further explored in future work. In addition, some related pre-clinical assessments should be also carried out.

In summary, our findings indicate that LncRNA H19 facilitates LPS-induced WI-38 cell pyroptosis via the miR-22-3p/NLRP3 axis. Our data provide a promising predictive and therapeutic target for pneumonia.

Disclosure of conflict of interest

None.

Address correspondence to: Wei Ji, Department of Pediatric Pulmonology, Children's Hospital of Soochow University, No. 303 Jingde Road, Suzhou 215003, Jiangsu Province, China. Tel: +86-0512-80693588; E-mail: szdxjiwei@163.com

References

[1] Zhang J, Mao F, Zhao G, Wang H, Yan X and Zhang Q. Long non-coding RNA SNHG16 promotes lipopolysaccharides-induced acute pneumonia in A549 cells via targeting miR-370-3p/IGF2 axis. Int Immunopharmacol 2020; 78: 106065.

[2] Zhou Z, Zhu Y, Gao G and Zhang Y. Long non-coding RNA SNHG16 targets miR-146a-5p/CCL5 to regulate LPS-induced WI-38 cell apoptosis and inflammation in acute pneumonia. Life Sci 2019; 228: 189-197.

[3] Yu HJ, Li H, Zhang Q, Shao Y and Wang YJ. Porous Co-MOF for cyanosilylation reaction and protective effect in child bronchial pneumonia by reducing the inflammatory response and IL-12 production in immune cells. Inorganica Chim Acta 2020; 503: 119426.

[4] Mylotte JM. Nursing home-associated pneumonia, part II: etiology and treatment. J Am Med Dir Assoc 2020; 21: 315-321.

[5] Guo J and Cheng Y. MicroRNA-1247 inhibits lipopolysaccharides-induced acute pneumonia in A549 cells via targeting CC chemokine ligand 16. Biomed Pharmacother 2018; 104: 60-68.

[6] Gong W, Shi Y and Ren J. Research progresses of molecular mechanism of pyroptosis and its related diseases. Immunobiology 2020; 225: 151884.

[7] Robinson N, Ganesan R, Hegedűs C, Kovács K, Kufer TA and Virág L. Programmed necrotic cell death of macrophages: focus on pyroptosis, necroptosis, and parthanatos. Redox Biol 2019; 26: 101239.

[8] Imre G. The involvement of regulated cell death forms in modulating the bacterial and viral pathogenesis. Int Rev Cell Mol Biol 2020; 353: 211-253.

[9] Han C, Yang Y, Yu A, Guo L, Guan Q, Shen H and Jiao Q. Investigation on the mechanism of mafenide in inhibiting pyroptosis and the release of inflammatory factors. Eur J Pharm Sci 2020; 147: 105303.

[10] Yu ZW, Zhang J, Li X, Wang Y, Fu YH and Gao XY. A new research hot spot: the role of NLRP3 inflammasome activation, a key step in pyroptosis, in diabetes and diabetic complications. Life Sci 2020; 240: 117138.

[11] Ying Y, Mao Y and Yao M. NLRP3 inflammasome activation by MicroRNA-495 promoter methylation may contribute to the progression of acute lung injury. Mol Ther Nucleic Acids 2019; 18: 801-814.

[12] Liu Y, Xu L, Lu B, Zhao M, Li L, Sun W, Qiu Z and Zhang B. LncRNA H19/microRNA-675/PPARα axis regulates liver cell injury and energy metabolism remodelling induced by hepatitis B X protein via Akt/mTOR signalling. Mol Immunol 2019; 116: 18-28.

[13] Liu S, Qiu J, Tang X, Cui H, Zhang Q and Yang Q. LncRNA-H19 regulates cell proliferation and invasion of ectopic endometrium by targeting ITGB3 via modulating miR-124-3p. Exp Cell Res 2019; 381: 215-222.

[14] Ye Y, Guo J, Xiao P, Ning J, Zhang R, Liu P, Yu W, Xu L, Zhao Y and Yu J. Macrophages-induced long noncoding RNA H19 up-regulation triggers and activates the miR-193b/MAPK1 axis and promotes cell aggressiveness in hepatocellular carcinoma. Cancer Lett 2020; 469: 310-322.

[15] Zhou Y, Fan RG, Qin CL, Jia J, Wu XD and Zha WZ. LncRNA-H19 activates CDC42/PAK1 pathway to promote cell proliferation, migration and invasion by targeting miR-15b in hepatocellular carcinoma. Genomics 2019; 111: 1862-1872.

[16] Liu M, Han T, Shi S and Chen E. Long noncoding RNA HAGLROS regulates cell apoptosis and autophagy in lipopolysaccharides-induced WI-38 cells via modulating miR-100/NF-κB axis. Biochem Biophys Res Commun 2018; 500: 589-596.

[17] Dong SM, Cui JH, Zhang W, Zhang XW, Kou TC, Cai QC, Xu S, You S, Yu DS, Ding L, Lai JH, Li M and Luo KJ. Inhibition of translation initiation factor eIF4A is required for apoptosis mediated by Microplitis bicoloratus bracovirus. Arch Insect Biochem Physiol 2017; 96.

[18] Nakai K, Karita S, Igarashi J, Tsukamoto I, Hirano K and Kubota Y. COA-Cl prevented TGF-β1-induced CTGF expression by Akt dephosphorylation in normal human dermal fibroblasts, and it attenuated skin fibrosis in mice models of systemic sclerosis. J Dermatol Sci 2019; 94: 205-212.

[19] Li M, Pang Z, Xiao W, Liu X, Zhang Y, Yu D, Yang M, Yang Y, Hu J and Luo K. A transcriptome analysis suggests apoptosis-related signaling pathways in hemocytes of Spodoptera litura after parasitization by Microplitis bicoloratus. PLoS One 2014; 9: e110967.

[20] Pei G, Xu L, Huang W and Yin J. The protective role of microRNA-133b in restricting hippocampal neurons apoptosis and inflammatory injury in rats with depression by suppressing CTGF. Int Immunopharmacol 2020; 78: 106076.

[21] Jia X, Cao B, An Y, Zhang X and Wang C. Rapamycin ameliorates lipopolysaccharide-induced acute lung injury by inhibiting IL-1β and IL-18 production. Int Immunopharmacol 2019; 67: 211-219.

[22] Wan P, Su W, Zhang Y, Li Z, Deng C, Li J, Jiang N, Huang S, Long E and Zhuo Y. LncRNA H19 initiates microglial pyroptosis and neuronal death in retinal ischemia/reperfusion injury. Cell Death Differ 2020; 27: 176-191.

[23] Louvrier C, Assrawi E, El Khouri E, Melki I, Copin B, Bourrat E, Lachaume N, Cador-Rousseau B, Duquesnoy P, Piterboth W, Awad F, Jumeau C, Legendre M, Grateau G, Georgin-Lavialle S, Karabina SA, Amselem S and Giurgea I. NLRP3-associated autoinflammatory diseases: phenotypic and molecular characteristics of germline versus somatic mutations. J Allergy Clin Immunol 2020; 145: 1254-1261.

[24] Xiang X, Mei H, Qu H, Zhao X, Li D, Song H, Jiao W, Pu J, Huang K, Zheng L and Tong Q. miRNA-584-5p exerts tumor suppressive functions in human neuroblastoma through repressing transcription of matrix metalloproteinase 14. Biochim Biophys Acta 2015; 1852: 1743-1754.

[25] Razakamanana MV, Audibert M, Andrianantoandro T and Harimanana A. Impact and efficiency of the integration of diagnosis and treatment of pneumonia in malaria community case management in madagascar. Work Pap 2017; 13: 238-249.

[26] Wang W, Lou C, Gao J, Zhang X and Du Y. LncRNA SNHG16 reverses the effects of miR-15a/16 on LPS-induced inflammatory pathway. Biomed Pharmacother 2018; 106: 1661-1667.

[27] Ning JZ, He KX, Cheng F, Li W, Yu WM, Li HY, Rao T and Ruan Y. Long non-coding RNA MEG3 promotes pyroptosis in testicular ischemia-reperfusion injury by targeting MiR-29a to modulate PTEN expression. Front Cell Dev Biol 2021; 9: 671613.

[28] She Q, Shi P, Xu SS, Xuan HY, Tao H, Shi KH and Yang Y. DNMT1 methylation of LncRNA GAS5 leads to cardiac fibroblast pyroptosis via affecting NLRP3 axis. Inflammation 2020; 43: 1065-1076.

[29] Yang F, Qin Y, Lv J, Wang Y, Che H, Chen X, Jiang Y, Li A, Sun X, Yue E, Ren L, Li Y, Bai Y and Wang L. Silencing long non-coding RNA Kcnq1ot1 alleviates pyroptosis and fibrosis in diabetic cardiomyopathy. Cell Death Dis 2018; 9: 1000.

[30] Wu LM, Wu SG, Chen F, Wu Q, Wu CM, Kang CM, He X, Zhang RY, Lu ZF, Li XH, Xu YJ, Li LM, Ding L, Bai HL, Liu XH, Hu YW and Zheng L. Atorvastatin inhibits pyroptosis through the lncRNA NEXN-AS1/NEXN pathway in human vascular endothelial cells. Atherosclerosis 2020; 293: 26-34.

[31] Liu Y, Xu XY, Shen Y, Ye CF, Hu N, Yao Q, Lv XZ, Long SL, Ren C, Lang YY and Liu YL. Ghrelin protects against obesity-induced myocardial injury by regulating the lncRNA H19/miR-29a/IGF-1 signalling axis. Exp Mol Pathol 2020; 114: 104405.

[32] Li B, Luan S, Chen J, Zhou Y, Wang T, Li Z, Fu Y, Zhai A and Bi C. The MSC-derived exosomal lncRNA H19 promotes wound healing in diabetic foot ulcers by upregulating PTEN via MicroRNA-152-3p. Mol Ther Nucleic Acids 2020; 19: 814-826.

[33] Nazarov PV, Reinsbach SE, Muller A, Nicot N, Philippidou D, Vallar L and Kreis S. Interplay of microRNAs, transcription factors and target genes: linking dynamic expression changes to function. Nucleic Acids Res 2013; 41: 2817-2831.

[34] Nappi L and Nichols C. MicroRNAs as biomarkers for germ cell tumors. Urol Clin North Am 2019; 46: 449-457.

[35] Xi X, Yao Y, Liu N and Li P. MiR-297 alleviates LPS-induced A549 cell and mice lung injury via targeting cyclin dependent kinase 8. Int Immunopharmacol 2020; 80: 106197.